

# Sustained Low-Level IFN- $\gamma$ Drives Mitochondrial Complex I Dysfunction and Macrophage Dysregulation in Lupus Nephritis

Hiroshi Tanaka<sup>1</sup>, Yuki Sato<sup>1\*</sup>, Kenji Mori<sup>2</sup>, Rina Okabe<sup>1</sup>, Takashi Ito<sup>2</sup>

<sup>1</sup>Department of Clinical Medicine and Innovation Research, University of Tokyo, Tokyo, Japan.

<sup>2</sup>Department of Translational Healthcare Sciences, Kyoto University, Kyoto, Japan.

## Abstract

The pathogenesis of autoimmune conditions is known to be significantly influenced by both macrophage dysregulation and mitochondrial malfunction. Nevertheless, the precise pathways that couple these two elements remain inadequately defined. We propose in this study that a sustained, low-grade presence of interferon-gamma (IFN- $\gamma$ ) acts as a pivotal mediator in these events. To examine this, experiments were conducted using ARE-Del mice, a strain that displays enduring, low-level IFN- $\gamma$  production alongside features characteristic of lupus nephritis (LN). Investigation of gene expression as a function of age and tissue type in these mice revealed pronounced downregulation of mitochondrial complex I subunits and their associated functions, particularly in renal tissue. The suppression of mitochondrial complex I linked to the mouse genotype signifies an initial defect that precipitates macrophage dysfunction. Of particular interest, the induction of remission in NZB/W lupus-prone mice led to a recovery of mitochondrial complex I gene expression and a correction of macrophage dysfunction in kidney-derived macrophages. Collectively, these observations imply that sustained, low-concentration IFN- $\gamma$  impairs mitochondrial complex I function in macrophages, underscoring its role in the incipient stages of autoimmune disorders such as lupus nephritis. This work yields a novel understanding of the molecular dialogues that are fundamental to autoimmune development and points toward possible therapeutic entry points.

**Keywords:** Interferon gamma, Mitochondrial complex I, Macrophage dysfunction, Lupus nephritis, Autoimmune diseases

**Corresponding author:** Yuki Sato  
**E-mail:** [yuki.sato@gmail.com](mailto:yuki.sato@gmail.com)

**How to Cite This Article:** Tanaka H, Sato Y, Mori K, Okabe R, Ito T. Sustained Low-Level IFN- $\gamma$  Drives Mitochondrial Complex I Dysfunction and Macrophage Dysregulation in Lupus Nephritis. Bull Pioneer Res Med Clin Sci. 2024;4(1):201-12. <https://doi.org/10.51847/s1aAndrYLe>

## Introduction

A growing body of evidence positions macrophage dysfunction as a principal driver of the etiology of autoimmune disorders, including rheumatoid arthritis (RA) and systemic lupus erythematosus (SLE) [1, 2]. Macrophages are broadly categorized into two dominant phenotypic groups: M1 and M2 [3, 4]. M1 macrophages, which become activated upon exposure to IFN- $\gamma$  and microbial components, adopt a pro-inflammatory

phenotype and release cytokines such as tumor necrosis factor-alpha (TNF- $\alpha$ ), interleukin-1 beta (IL-1 $\beta$ ), interleukin-6 (IL-6), and interleukin-12 (IL-12). These molecules facilitate pathogen eradication and amplify inflammatory cascades. In contrast, M2 macrophages play an anti-inflammatory and tissue remodeling role, producing mediators such as interleukin-10 (IL-10) and transforming growth factor beta (TGF- $\beta$ ). They are also implicated in promoting the proliferation and function of regulatory T cells (Tregs), thereby reinforcing immune

tolerance and resolving inflammation [5]. An equilibrium skewed toward M1 over M2 polarization is a commonly reported feature across a spectrum of autoimmune conditions [6]. However, contemporary insights reveal that, despite this polarized imbalance, it is the intrinsically aberrant function of macrophages—encompassing defective intracellular signaling pathways and compromised dialogue with Tregs—that exerts a more decisive influence on disease progression [7].

Mitochondria serve as master regulators of immune cell bioenergetics, and a growing consensus identifies mitochondrial dysfunction as a fundamental trigger of autoimmune pathology in conditions such as RA, SLE, and Sjögren's syndrome [8-10]. Reactive oxygen species (ROS) of mitochondrial origin, generated amidst inflammatory insults, can provoke oxidative damage to mitochondrial DNA (mtDNA) [11]. Once oxidized, mtDNA escapes into the cytoplasm and engages innate immune detectors, namely cyclic GMP-AMP Synthase-Stimulator of Interferon Genes (cGAS-STING) and Toll-like receptor 7 (TLR7), triggering a cascade that culminates in the synthesis of type I interferons (IFNs) [12, 13]. This uncontrolled reinforcement of type I IFN signaling forges a self-amplifying loop, magnifying inflammatory outputs and entrenching chronic inflammation—a signature of autoimmune disorders [14, 15]. In addition, protracted inflammatory states can impede the metabolic reprogramming required for macrophages to transition from a pro-inflammatory M1 to a reparative M2 identity [16]. The failure of this metabolic handover deepens macrophage impairment, sustaining the chronic inflammatory milieu typical of long-standing autoimmune disease. Still, these inferences await further empirical consolidation.

The mitochondrial respiratory chain comprises an array of protein assemblies (complexes I through IV) and the ATP-generating synthase (complex V) embedded within the inner mitochondrial membrane, all of which directly participate in oxidative phosphorylation (OXPHOS) [17]. Complex I, also designated NADH: ubiquinone oxidoreductase, occupies a crucial position by shuttling electrons from NADH to ubiquinone, thereby initiating the electron transport sequence. An attenuation of complex I activity can disrupt the orderly flow of electrons, leading to a shortfall in cellular energy currency. Such a disruption in mitochondrial function, especially within the electron transport chain (ETC), is thought to contribute to metabolic dysregulation associated with obesity and the development of insulin resistance [18]. Our team's recent publication documented that curtailing mitochondrial complex I activity is instrumental in obesity-driven, chronic inflammation mediated by inter-organ crosstalk between the liver and adipose depots [19, 20]. In light of the widely accepted role of mitochondrial compromise in

the pathogenesis of major autoimmune entities such as type 1 diabetes (T1D), RA, multiple sclerosis (MS), and SLE [21, 22], it stands to reason that an analogous chronic inflammatory circuit might likewise drive the genesis of autoimmunity.

IFN- $\gamma$  is a principal cytokine that commits macrophages to the M1 lineage, driving their pro-inflammatory programming [23]. As a key product of Th1 cells, IFN- $\gamma$  is implicated in the initiation and propagation of diverse autoimmune diseases, including RA, SLE, and T1D [24, 25]. That said, a complete picture of its mechanistic contributions has yet to emerge. The operational status of mitochondrial complex I is a foundational requirement for mounting an IFN- $\gamma$  response, as revealed by CRISPR-Cas9 genetic screens that distinguished its role from that of other respiratory chain components [26]. Conversely, subjecting macrophages to IFN- $\gamma$  induces a metabolic realignment, characterized by a downshift in OXPHOS and an upregulation of anaerobic glycolysis to foster rapid ATP generation [27]. This metabolic pivot is indispensable for Th1 cell activation and simultaneously suppresses M2 macrophage differentiation [28]. Owing to the layered complexity of immune interactions and the pleiotropic character of signaling networks, further dissection is imperative to unravel the operative mechanisms and their bearing on disease.

ARE-Del mice, engineered to exhibit a systemic, persistent low-level IFN- $\gamma$  output due to modifications within the AU-rich elements of the 3'-untranslated region (UTR), spontaneously manifest autoimmune syndromes mirroring LN and primary biliary cirrhosis (PBC) [29, 30]. Perturbations in the AU-rich elements of the IFN- $\gamma$  gene's 3'-UTR give rise to a systemic, low-grade but continuous IFN- $\gamma$  signal that synergizes with type I interferon pathways, consequently intensifying autoimmune pathology [31]. Macrophage dysfunction, typified by excessive oxidative burden and defective fatty acid oxidation, is thought to be a central pathogenic mechanism in these disease states [32]. Evidence of a depressed NAD<sup>+</sup>/NADH ratio in myocytes harvested from ARE-Del mice indicates impaired mitochondrial complex I activity, leading to metabolic derangement, compromised energy output, and elevated oxidative stress, all of which contribute to cardiomyopathy [33]. Hence, deploying this murine model warrants a deeper inquiry to delineate the contribution of mitochondrial complex I to macrophage functional failure and its involvement in autoimmune pathogenesis.

Here, our central objective was to ascertain whether the sustained presence of IFN- $\gamma$  cripples mitochondrial complex I, with a specific focus on macrophages residing in the kidneys of ARE-Del mice, and to posit this crippling effect as a cornerstone in the development of LN. Our investigation centered on the concept that mitochondrial

complex I impairment may impede a crucial metabolic transition in macrophages, thereby inducing their dysfunction. Furthermore, we sought to determine the concordance of these results with other lupus-prone mouse strains and human clinical datasets, thus corroborating the translational relevance of our discoveries across disparate experimental and clinical landscapes.

## Materials and Methods

### *Gene expression of ARE-Del<sup>-/-</sup> mice*

The ARE-Del<sup>-/-</sup> mouse line harbors a deletion spanning a 162-nucleotide segment within the AU-rich element (ARE) region of the IFN- $\gamma$  gene's 3'UTR. This alteration yields constitutively low but steady serum IFN- $\gamma$  concentrations. We have specifically cataloged phenotypic similarities to the autoimmune disorders LN and PBC, which arise in the kidney and liver, respectively [29, 30]. Consistent with our earlier methodology, RNA was harvested from spleen, thymus, kidney, and blood to delineate tissue- and age-dependent transcriptomic signatures shaped by genotype (ARE-Del homozygotes and heterozygotes) [32]. The experimental framework, based on a minimum of 3 biological replicates, used material from both homozygous and heterozygous ARE-Del mice at 3, 6, and 12 weeks of age. These were measured against samples from control littermates and hybridized onto a custom Agilent microarray designated Agilent-026855 (Agilent Technologies, Santa Clara, CA, USA). This platform contained 39,488 unique probes and was run following the manufacturer's specifications. The downstream analysis employed log<sub>2</sub>-transformed intensities, normalized at the array level to preserve a uniform signal distribution. Statistical assessment of differential gene expression among groups was performed using ANOVA (Analysis of Variance) within Partek Genomics Suite 6.6 (v6.14.006). The source data analyzed here have been deposited in NCBI's Gene Expression Omnibus (GEO) under accession GSE248465.

### *Renal macrophage data acquisition*

To validate the premise that complex I inhibition is key to derailing macrophage function in the kidneys of ARE-Del<sup>-/-</sup> mice, we undertook a comparative transcriptomic evaluation of the GSE27045 dataset. As outlined by Bethunaickan *et al.*, kidney macrophages at different nephritis stages were sorted via flow cytometry: F4/80(hi) cells were isolated during the early nephritis window (control), the active nephritis window (sick), and following remission induction (remission) from the kidneys of nephritic NZB/W mice [34]. Specimens originated from mice aged 8 to 16 weeks (n = 6) representing the early stage, mice at 2 to 6 weeks after proteinuria onset but before reaching terminal renal failure

(n = 7), and mice 3 to 4 weeks after achieving full remission after one cyclophosphamide injection paired with six doses of CTLA4Ig and anti-CD154 (n = 4). RNA extracted from the purified cells was hybridized on the Affymetrix GeneChip® Mouse Genome 430 2.0 array (Affymetrix, Santa Clara, CA, USA). Differential expression analysis was conducted using GEO2R, applying a t-test to assess the significance of differences between the two group means.

### *Pre-ranked GSEA*

The utility of a pre-ranked Gene Set Enrichment Analysis (GSEA) strategy for mechanistic interrogation has been borne out by our team's earlier obesity-focused studies [19, 20]. Fundamentally, this approach orders transcriptional profiles by fold-change rank and then applies the GSEA computational framework to detect enrichment signals within curated gene collections, yielding two primary statistical measures: Normalized Enrichment Scores (NESs) alongside Enrichment Scores (ESs). Several complementary statistical filters are conventionally applied when assessing the robustness of pre-ranked GSEA outputs—these include a nominal-corrected P-value, a False Discovery Rate (FDR) metric, and Family-Wise Error Rate (FWER) control, with the accepted boundaries for each typically set at or below 0.05. The FWER metric serves as a stringent correction, controlling the likelihood that even a single false positive arises from the multiplicity of tests. Our own determinations of significance rested upon the FDR, and in situations where the computation yielded a raw value of “0,” a substitute floor of  $1 \times 10^{-6}$  was inserted to permit logarithmic conversion. Previous reports from our laboratory relied heavily on a classical analytical framework for inference. Yet, given the more pronounced transcriptional responses observed in ARE-Del<sup>-/-</sup> animals, a weighted approach was selected to assess the relevance of these shifts. Because weighted analysis places greater emphasis on variation at the level of individual genes, significance estimates can appear inflated; simultaneously, NES magnitudes often fall short of those obtained through classical analysis, a pattern that demands careful interpretive judgment.

### *Acquisition of scRNA-seq data from kidney specimens of patients with LN*

A key objective was to evaluate the extent to which signatures identified in murine lupus models translate to clinical settings, prompting our analysis of single-cell RNA sequencing (scRNA-seq) profiles from renal biopsies of LN patients. These data were accessed through two online analytical portals: <https://immunogenomics.io/ampsle> (accessed on 23 September 2024) and

[https://portals.broadinstitute.org/single\\_cell/study/amp-phase-1](https://portals.broadinstitute.org/single_cell/study/amp-phase-1) (accessed on 23 September 2024) [35]. Based on the specimen handling and data generation workflow published by Arazi, A. *et al.*, kidney tissue was harvested from 24 LN patients and supplemented with 10 control biopsy samples from living kidney donors. Single-cell sequencing libraries were prepared using a modified CEL-Seq2 protocol, and the resulting libraries were run on the Illumina HiSeq 2500 system (Illumina, San Diego, CA, USA). Read mapping to the hg19 human reference assembly was performed using the Spliced Transcripts Alignment to a Reference (STAR) pipeline.

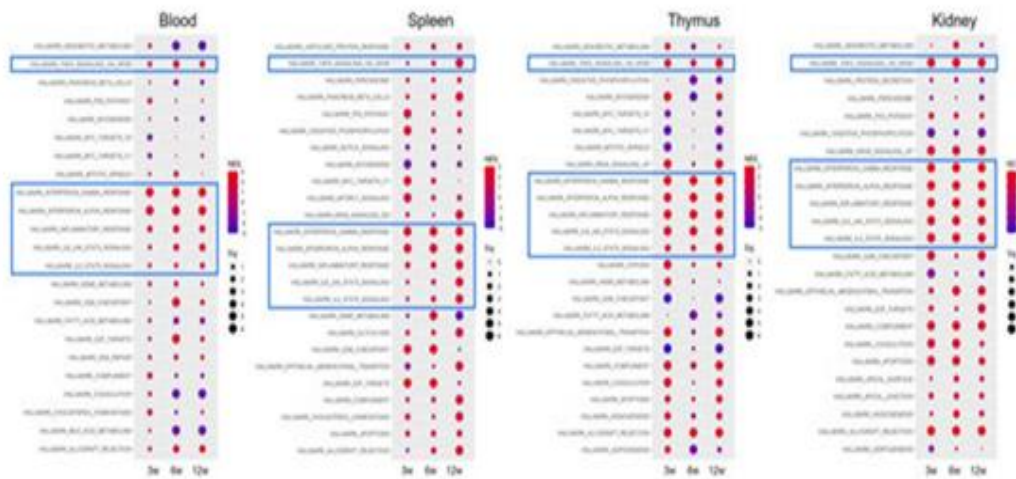
### Data visualization with R

For the bulk of data visualization tasks, we operated within the R programming ecosystem, using R-4.3.1, and relied on RStudio (version 2022.12.0 + 353) as the primary development interface. The rich graphical capabilities afforded by add-on libraries—most notably *ggplot2* (version 3.5.1) and *heatmap2*, the latter sourced from the *gplots* package (version 3.1.3)—enabled us to produce an extensive array of both analytically revealing and visually polished figures.

## Results and Discussion

### Distinct age- and tissue-dependent hallmark gene set expression in ARE-Del/- mice

Pre-ranked GSEA was utilized to probe how hallmark gene sets shifted with age in a tissue-specific manner (**Figure 1a**). Although diverging signatures emerged across the various tissues—highlighted by the blue rectangles—a unifying, statistically robust association with IFN- $\gamma$  responses and accompanying inflammatory cascades was repeatedly identified, a pattern reminiscent of findings from obesity studies. The pre-ranked GSEA approach yielded more temporally consistent outputs than those derived from Enrichr-based analysis of DEGs [32]. A noteworthy observation was the presence of distinctive alterations at the 6-week mark uniformly across all tissues, a feature captured by both analytical strategies. This consistent signature hints at a conduit linking renal inflammatory events to broader immune dynamics via the circulatory system. Tissue-level divergence was further reflected in the IFN- $\gamma$  response gene expression landscapes shown in **Figure 1b**. When scrutinizing within-tissue trajectories, the kidney mounted a particularly intense IFN- $\gamma$  response. The blood and spleen shared broadly analogous expression patterns, whereas the thymus and kidney showed higher levels of IFN- $\gamma$ -responsive gene expression.



a)

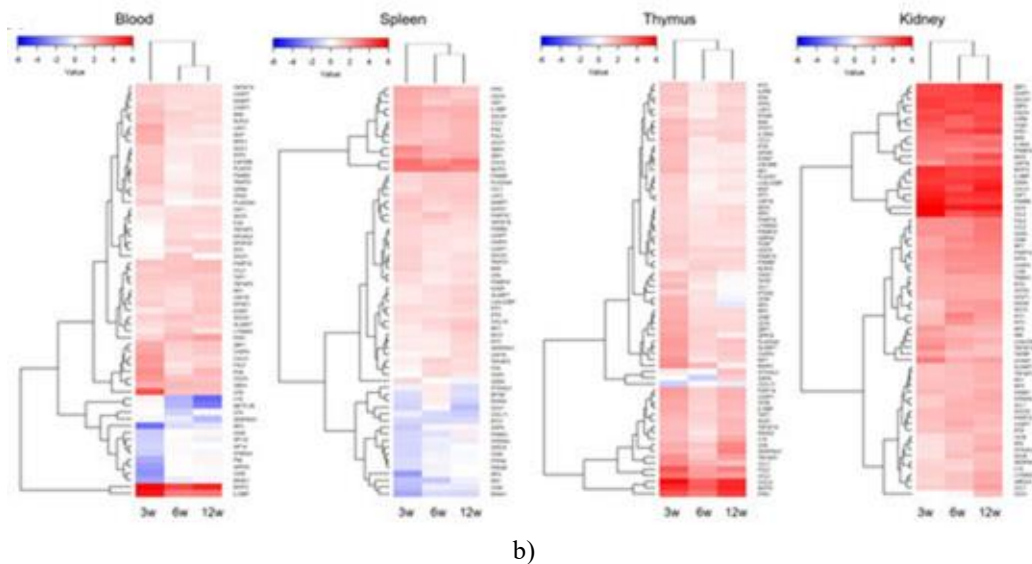
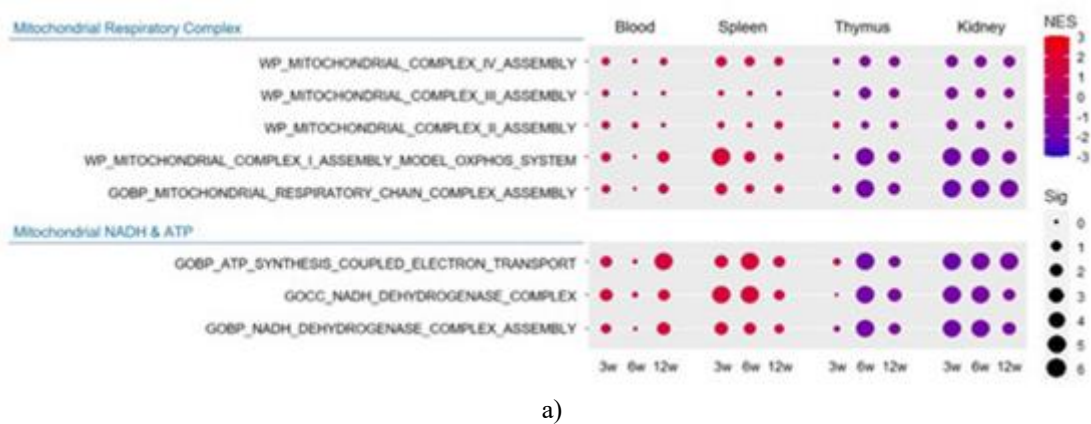


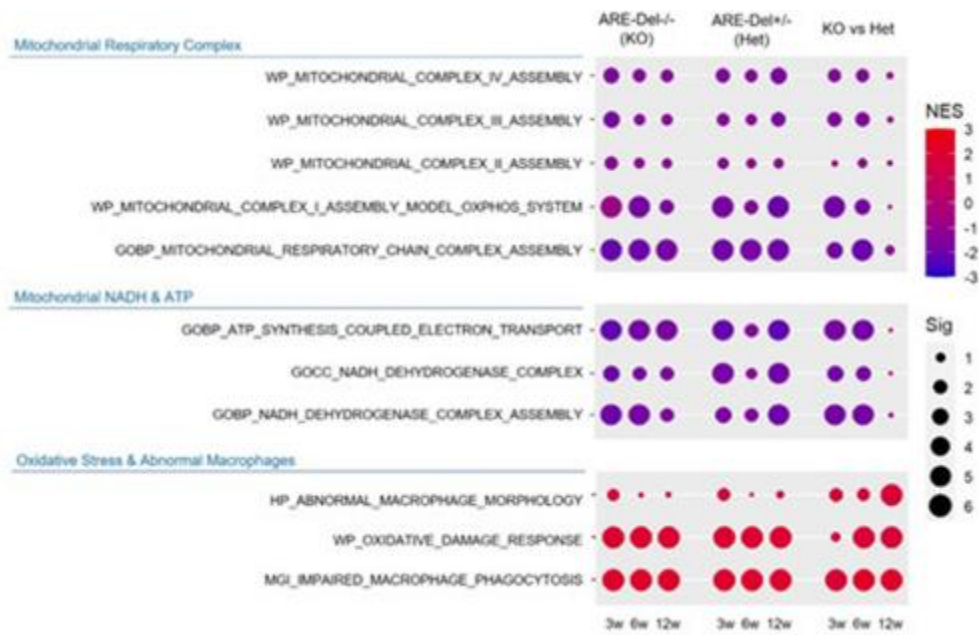
**Figure 1.** Time- and tissue-dependent hallmark gene set analysis using pre-ranked GSEA in ARE-Del-/- mice over time: (a) Hallmark gene set analysis conducted at the 3-, 6-, and 12-week time points within blood, spleen, thymus, and kidney samples obtained from ARE-Del-/- mice. The dimensions of each plotted dot are scaled to reflect the degree of significance (Sig), expressed as  $-\log_{10}(\text{FDR } q\text{-value})$ , while dot coloring is tied to the NES. Inflammatory signatures that overlap across conditions are outlined with blue rectangles. **\*(b)\*** Heatmaps depicting the expression patterns of IFN- $\gamma$  response genes at the 3-, 6-, and 12-week intervals, surveyed across blood, spleen, thymus, and kidney tissues isolated from ARE-Del-/- mice.

*Positive correlation between suppressed mitochondrial complex I activity and macrophage dysfunction in the kidney of ARE-Del-/- mice*

**Figure 2a** depicts how mitochondrial complex operations shift with age in a tissue-dependent fashion. Among complexes I through IV, the kidney showed the most pronounced decline in complex I activity across all time windows, while the thymus registered a meaningful

decline only after the 6-week point. In a departure from this trend, blood and spleen samples showed the opposite pattern for complex I activity, though the statistical weight of this observation remained relatively modest. Corroboration of these effects came from pathway-level analyses focused on mitochondrial NADH and ATP dynamics, such as the coupling of ATP synthesis to electron transport and the assembly of the NADH dehydrogenase complex.





b)

**Figure 2.** Dysregulated mitochondrial complex I activity in the kidney of ARE-Del<sup>-/-</sup> mice: (A)\*\* Tissue-dependent suppression of mitochondrial complex I activity in ARE-Del<sup>-/-</sup> mice. A series of dot plots showing enrichment signals across gene sets for the mitochondrial respiratory chain and NADH/ATP-linked processes, examined in blood, spleen, thymus, and kidney tissues collected at the 3-, 6-, and 12-week time points. The size of each dot is proportional to the level of significance (Sig.), computed as  $-\log_{10}(\text{FDR } q\text{-value})$ , whereas the color assigned to each dot corresponds to the NES value. \*\*(B)\*\* Comparison of mitochondrial complex I activity in the kidneys between ARE-Del<sup>-/-</sup> and ARE-Del<sup>+/-</sup> mice at 3, 6, and 12 weeks of age. Dot plots summarizing the enrichment landscape for gene sets connected to the mitochondrial respiratory complex, NADH- and ATP-related processes, oxidative stress pathways, and signatures of aberrant macrophage function. Significance (Sig), depicted as  $-\log_{10}(\text{FDR } q\text{-value})$ , is conveyed through dot size, and NES is mapped onto dot color. The column groupings represent distinct enrichment contrasts: KOs (ARE-Del<sup>-/-</sup> vs. control littermates), Hets (ARE-Del<sup>+/-</sup> vs. control littermates), and KOs vs. Hets (ARE-Del<sup>-/-</sup> vs. ARE-Del<sup>+/-</sup>).

We next compared the transcriptomic profiles of ARE-Del homozygotes (ARE-Del<sup>-/-</sup>) and heterozygotes (ARE-Del<sup>+/-</sup>) using pre-ranked GSEA. **Figure 2b** charts a temporal comparison between these genotypes. The initial set of three columns tracks shifts over time in ARE-Del homozygotes (KOs), the middle three columns do the same for heterozygotes (Hets), and the final three columns contrast the two directly across the time course (KOs vs. Hets). The dampening of complex I activity emerged as the most severely impacted parameter in both genetic groups, and this response was already underway from the earliest phase examined. The magnitude of early suppression was greater in homozygotes relative to heterozygotes. However, the distinction between genotypes had largely faded by the 12-week point, pointing to a plateau of maximal suppression in both cohorts.

#### *Similarity of hallmark gene sets between renal inflammation in ARE-Del<sup>-/-</sup> Mice and isolated renal macrophages from NZB/W lupus-prone mice*

Operating under the assumption that a decline in mitochondrial complex I activity represents the earliest

step toward renal mitochondrial breakdown, we anticipated that comparable molecular fingerprints would be detectable in isolated kidney macrophages from a separate lupus-prone strain. To put this idea to the test, transcriptional data were analyzed, as outlined in Section 4, from F4/80(hi) macrophages sorted from the kidneys of NZB/W lupus-prone mice at three distinct disease stages: pre-autoimmunity baseline (G2\_Control), full-blown active lupus nephritis (G1\_Sick), and after pharmacological induction of remission (G3\_Remission). As shown in **Figure 3a**, the hallmark gene set comparison between G1 and G2 revealed a generally positive enrichment landscape in the kidney that paralleled observations in ARE-Del<sup>-/-</sup> mice, most notably for IFN- $\gamma$  and related inflammatory programs. On the flip side, remission—elicited by a single cyclophosphamide injection complemented by six rounds of CTLA4Ig/anti-CD154 treatment—shifted the macrophage transcriptome toward negatively enriched gene sets rooted in the IFN- $\gamma$  response. As shown by the blue square in **Figure 3a**, the enrichment trajectories for gene sets centered on IFN- $\gamma$ , IFN- $\alpha$ , TNF- $\alpha$ , and IL-6 signaling faithfully recapitulated the previously cataloged patterns in both obese subjects

and ARE-Del<sup>-/-</sup> mice (**Figure 3b**). The 20 most significantly perturbed genes in each gene set have been

highlighted, with red denoting elevated expression and blue denoting suppressed expression.

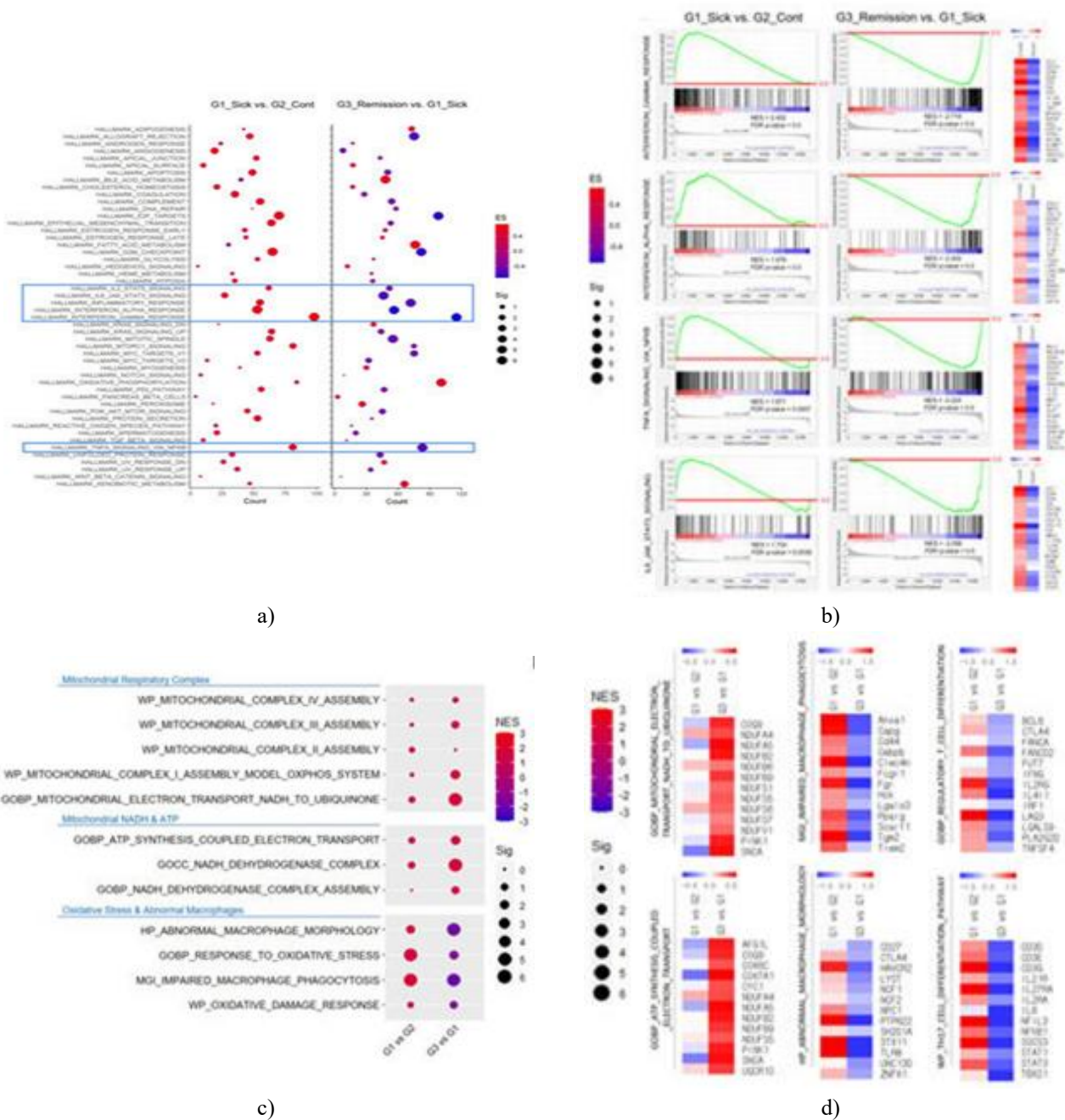


**Figure 3.** Recovery of inflammatory responses and complex I activity by remission in isolated renal macrophages from NZB/W lupus-prone mice: (a) Dot plots capturing alterations across hallmark gene sets, with side-by-side comparisons drawn between the G1\_Sick cohort (active lupus nephritis) and the G2\_Control cohort (lupus onset), as well as between the G3\_Remission cohort (status after remission induction) and the G1\_Sick cohort. 50 hallmark pathways are arrayed along the y-axis. The x-axis shows the number of genes meeting the enrichment significance threshold for each pathway, as determined by the GSEA algorithm. Dot dimensions convey significance measured as  $-\log_{10}(\text{FDR } q\text{-value})$ , whereas dot coloring maps to the ES—red reflecting a positive score, blue a negative one. (b) Representative GSEA-derived enrichment plots exhibiting positive scores for gene sets tied to IFN- $\gamma$ , IFN- $\alpha$ , IL-6, and TNF- $\alpha$  signaling, evaluated across both the G1 vs. G2 and G3 vs. G1 comparisons. The zero-crossing point (0.0) of the enrichment score is traced with a red line. The heatmaps alongside show expression magnitudes for the top-ranking enriched genes in each gene set, providing a visual means to contrast the two group pairings. (c) Dot plots reporting enrichment levels for gene sets about the mitochondrial respiratory complex, mitochondrial NADH and ATP processes, oxidative stress, and dysfunctional macrophage phenotypes, again comparing G1 vs. G2 and G3 vs. G1. (d) Heatmaps illustrating the expression intensities of

the most strongly enriched genes belonging to each respective gene set, allowing for direct comparison between the G1 vs. G2 and G3 vs. G1 groupings.

### *Recovery of suppressed complex I activity by remission in isolated renal macrophages from NZB/W lupus-prone mice*

Because the IFN- $\gamma$ -driven signatures identified in renal macrophages isolated from NZB/W lupus-prone mice closely recapitulated the alterations in macrophage-associated gene sets earlier documented in ARE-Del/- animals, we next performed a side-by-side evaluation of complex I performance and its downstream pathways at three distinct disease junctures in these isolated renal macrophages: the incipient stage of lupus, the florid active phase, and remission. It is worth emphasizing that the reference cohort employed here corresponds not to a disease-free state but to the earliest phase of lupus onset. We hypothesized that depression of complex I function likely occurs during the initial stages of pathogenesis, which would help explain the negligible difference between the active nephritis stage and the onset period. As illustrated in **Figure 3c**, the overall activity of mitochondrial complexes did not differ meaningfully between the G1 and G2 groups. Yet, when G3 was compared with G1, a specific gene set centered on complex I function showed positive enrichment. A more granular dissection of the pathways affected by complex I suppression revealed that the transcriptional programs altered in renal macrophages during the active disease phase, as shown in **Figure 3c**, underwent diametrically opposite regulation upon achieving remission. A concomitant decrease in the heightened aberrant macrophage signatures present during active lupus was also documented as the animals transitioned into remission. In parallel, a matching number of genes, selected based on the largest fold changes from the curated gene roster in **Figure 3c**, is presented in **Figure 3d**.

### *Suppressed mitochondrial complex I activity and macrophage dysfunction in a specific renal macrophage cluster of LN patients*

Single-cell RNA sequencing of kidney biopsy material from LN patients revealed a marked attenuation of mitochondrial complex I activity, localized to a discrete macrophage subset. To explore the relationship between IFN- $\gamma$  signaling and its possible contribution to autoimmune disease evolution, the transcriptional levels of IFNG, IFNGR1, IFNGR2, HLA-DPA1, and HLA-DPB1 were mapped across distinct cell clusters on a t-SNE plot. While IFNG expression was largely restricted to T cell clusters (T1, T2, T4, T5a), IFNGR2 was broadly distributed across B lymphocytes, endothelial cells, and macrophages, whereas IFNGR1 exhibited a selective enrichment within the macrophage compartment. Of

particular note, the macrophage-restricted expression signature of IFNGR1 closely matched the patterns observed for HLA-DPB1 and HLA-DPA1.

Gene sets associated with the assembly of mitochondrial complex I were prominently upregulated in epithelial cells (E0), activated B cells (B1), and dividing cells (D0). In stark contrast, these gene sets were suppressed in macrophages and T lymphocytes, with the M4 macrophage cluster exhibiting the most pronounced downregulation. The representative gene panel linked to ATP biosynthesis was also depressed in macrophages and T cells, with the M4 cluster showing the greatest reduction. Inside the M4 macrophage population, a pronounced upswing was detected for genes participating in cholesterol metabolism and for pathways connected to peroxisome proliferator-activated receptor gamma (PPARG). Furthermore, the M4 cluster showed maximal expression levels of chemokine (C-C motif) ligand 2 (CCL2) and Fc gamma receptor I A (FCGR1A), suggesting that M4 macrophages are primed to mount an exaggerated inflammatory response.

In the present study, which addresses LN pathogenesis, we showed that persistent, low-grade IFN- $\gamma$  provokes a lasting repression of genes encoding mitochondrial complex I subunits and their associated enzymatic activities, manifesting in a tissue-selective manner within the renal compartment. This early-appearing perturbation was accompanied by alterations in the mitochondrial translational apparatus, a phenomenon that may further intensify mitochondrial compromise in concert with metabolic disequilibrium. These results were corroborated by parallel findings in renal macrophages isolated from lupus-prone mouse strains and in specific macrophage subpopulations delineated via single-cell transcriptomic analysis of LN patient specimens. Grounded in the evidence outlined above, the ensuing discussion will address the mechanisms by which IFN- $\gamma$  can inhibit complex I and, critically, how this specific mechanism can dysregulate macrophage function.

Under inflammatory conditions, a metabolic reconfiguration—whereby OXPHOS is displaced by glycolytic metabolism—empowers macrophages to swiftly produce energy and biosynthetic precursors that are essential for sustaining inflammatory functions and operating effectively within a hostile tissue milieu [28]. Although sustained IFN- $\gamma$  signaling may initially depend upon mitochondrial complex I engagement, the progressive intensification of inflammatory cascades can transform its suppression into a driver of the OXPHOS-to-glycolysis shift. In contrast to type II IFNs, type I IFNs are understood to be reliant on OXPHOS and fatty acid

oxidation (FAO) for their energetic supply. This requirement is especially pronounced in plasmacytoid dendritic cells (pDCs) and cells of non-hematopoietic origin [36]. Set against this backdrop, the type I IFN surge elicited by IFN- $\gamma$  demands opposing metabolic configurations; nevertheless, the relentless suppression of OXPHOS and FAO within macrophages eventually manifests as aberrant cellular behavior. When one considers the ablation of the type I IFN receptor (Ifnar1) or TLR7—molecules that are distinctly tied to the female-predominant pathogenesis of PBC and LN in ARE-Del mice [30, 31]—the IFN- $\gamma$ -mediated amplification of type I IFNs appears to be linked with macrophage dysfunction. This relationship likely stems from the mitochondrial metabolic disequilibrium required for proper cellular function.

The same forces are at play in the metabolic demands required for the phenotypic transition from M1 to M2 macrophages, thereby further entrenching macrophage dysfunction. M2 macrophages draw primarily upon OXPHOS and FAO as their principal energy-generating pathways [37]. M1 macrophages, by comparison, are capable of rapidly mobilizing energy production—albeit at reduced efficiency—by rerouting metabolism from OXPHOS toward glycolysis. A profound OXPHOS suppression was evident in ARE-Del mice. In a similar vein, renal macrophages isolated from NZB/W lupus-prone mice displayed a striking depression of OXPHOS. Tellingly, within the CM4 cluster, which has been classified as an M2-like macrophage population based on single-cell sequencing data from LN patients, a notable decline in the expression of genes encoding mitochondrial complex I components and their functional activities was observed. Furthermore, our results suggest that the reciprocal regulatory interplay between IFN- $\gamma$  and PPAR- $\gamma$  (PPAR $\gamma$ ) operating within macrophages could be connected to breakdowns in the control of cholesterol trafficking and anti-inflammatory programs, both of which are interwoven with the metabolic mechanisms elaborated above. In sum, our data suggest that the metabolic reprogramming required to mount anti-inflammatory responses, exemplified by M2-type activation, may be a key contributor to macrophage dysfunction in the pathogenesis of lupus nephritis.

Moving beyond metabolic switching defects, the mechanistic landscape of macrophage dysfunction in ARE-Del mice incorporates several additional layers. Our earlier investigations established that rapamycin exposure disrupts autophagosome biogenesis in splenic macrophages isolated from ARE-Del $^{-/-}$  mice [32]. This disruption can be traced to impeded lysosomal localization of mTOR, an event that prevents mTOR from being activated by rapamycin and thereby derails the autophagosome assembly process [38]. This interpretation

is buttressed by observations that mTOR lysosomal positioning is blocked during the macrophage priming phase triggered by IFN- $\gamma$  [39]. Beyond this, compromised autophagosome generation can diminish the efficiency of DNA repair pathways [40, 41], culminating in elevated rates of cellular apoptosis or senescence in the face of the excessive oxidative burden imposed by inflammatory processes. Our dataset also reveals enrichment of gene sets associated with cell death mechanisms, spanning apoptosis and pyroptosis, as well as those related to cellular senescence. Accordingly, our findings suggest that faulty autophagosome formation in ARE-Del mice contributes to macrophage dysfunction and may play a role in the pathogenesis of autoimmune disorders.

The intertwining of autophagic malfunction and metabolic reprogramming defects constitutes a linked pathological circuit capable of propelling the initiation and worsening of numerous diseases, spanning from cancer to neurodegenerative conditions [42, 43]. Central to cellular housekeeping, the autophagic pathway is responsible for the breakdown and recycling of damaged organelles and aberrant protein aggregates. Should this surveillance system falter, the resulting accumulation of defective materials—mitochondria being a prime example—places substantial stress on the cell and disrupts its metabolic operations. This breakdown impairs the cell's ability to efficiently meet energy needs, redirecting it toward an unbalanced metabolic state that often manifests as glycolytic dependence despite ample oxygen availability (similar to the Warburg effect observed in malignant cells) [44]. Such a skewing of the metabolic switch can intensify the inflammatory backdrop typical of autoimmune states, as the rewired energy pathways galvanize immune cell activation, locking in a vicious cycle of inflammation paired with cellular decline. Considering published evidence that autophagic dysfunction may participate in the emergence of autoimmune disorders [45], this two-way exchange between defective autophagy and metabolic disequilibrium could be instrumental in both perpetuating and magnifying autoimmune disease processes.

Regarding the mechanistic pathway by which mitochondrial complex I depression leads to mitochondrial collapse in ARE-Del mice, published work indicates that when complex I function is curtailed, ATP synthesis declines. At the same time, ROS accumulate, triggering oxidative damage to mitochondrial structures and paving the way for NLRP3 inflammasome assembly [46–48]. Evidence of this sequence is found in the kidneys of ARE-Del $^{-/-}$  animals, where the persistent IFN- $\gamma$ -dependent repression of complex I aligns with elevated NLRP3 inflammasome engagement and pyroptotic cell death. In addition, because cGAS-STING and TLR7 are both recognized as upstream inducers of type I interferon expression, these signaling modules may further

contribute to NLRP3 inflammasome construction and amplify interferon signaling in ARE-Del mice. Mitochondrial injury or outright damage can permit the seepage of oxidized mtDNA into the cytoplasm, where it serves as a trigger for the cGAS-STING axis, fueling type I IFN output and robust inflammatory responses [49]. Along similar lines, TLR7 engagement triggers the release of type I IFNs and other pro-inflammatory factors, such as TNF- $\alpha$  and IL-6 [50]. Thus, sustained IFN- $\gamma$  exposure drives the M1 polarization trajectory, during which suppression of complex I heightens the oxidative burden, promotes mtDNA escape, and stimulates type I IFN production, all of which collectively advance the development of lupus.

Another critical insight emerging from our data is the coordinated expression of gene sets associated with mitochondrial complex I and the mitochondrial translation machinery. As specific ETC subunits are under the direct governance of mitochondrial translation [51], any suppression of this translation process stands to restrict further the generation of ETC elements—complex I included—thereby deepening mitochondrial impairment. Since TLR7 exhibits a binding preference for single-stranded RNA (ssRNA) ligands [52], a downregulation of mitochondrial translation activity might produce fragmented ssRNA molecules capable of activating TLR7, thereby contributing to LN pathogenesis. This suggests that oxidized ssRNA fragments might trigger innate immune pathways through mechanisms akin to those used by oxidized mtDNA.

## Conclusion

To summarize, the present work provides meaningful insights into the role of mitochondrial dysfunction in the pathogenesis of LN, underscoring how long-term, IFN- $\gamma$ -driven repression of mitochondrial complex I activity promotes metabolic disharmony, oxidative stress, and compromised macrophage function. The tandem regulation involving mitochondrial complex I and mitochondrial translation, alongside the generation of type I interferons and the mobilization of inflammatory platforms such as the NLRP3 inflammasome and TLR7 signaling, reveals the deeply interwoven links between mitochondrial failure and autoimmune reactions. These observations suggest that therapeutic strategies focused on modulating mitochondrial complex I function and restoring mitochondrial health may help counteract macrophage dysfunction and, by extension, slow the progression of LN and other autoimmune pathologies. Ongoing investigation into the crosstalk linking metabolic reprogramming, autophagic dysregulation, and immune signaling pathways will remain crucial for refining our comprehension of autoimmune pathogenesis and identifying novel therapeutic entry points.

**Acknowledgments:** None

**Conflict of interest:** Author Suntae Kim was employed by the company Omixplus, LLC. The remaining authors declare that the research was conducted in the absence of any commercial or financial relationships that could be construed as a potential conflict of interest.

**Financial support:** This research has received financial support from the National Research Foundation of Korea (Grant No. 2022H1D3A2A02081567, RS-2024-00342528, and RS-2023-00213596). Additionally, this project has been funded, in whole or in part, by federal intramural research programs of the National Cancer Institute, CCR, and CIL. The content of this publication does not necessarily reflect the views or policies of the U.S. Department of Health and Human Services, nor does mention of trade names, commercial products, or organizations imply endorsement by the U.S. Government.

**Ethics statement:** None

## References

1. Gerasimova EV, Popkova TV, Gerasimova DA, Kirichenko TV. Macrophage dysfunction in autoimmune rheumatic diseases and atherosclerosis. *Int J Mol Sci.* 2022;23(9):4513.
2. Ma C, Xia Y, Yang Q, Zhao Y. The contribution of macrophages to systemic lupus erythematosus. *Clin Immunol.* 2019;207:1–9.
3. Yunna C, Mengru H, Lei W, Weidong C. Macrophage M1/M2 polarization. *Eur J Pharmacol.* 2020;877:173090.
4. Wang N, Liang H, Zen K. Molecular mechanisms that influence the macrophage M1-M2 polarization balance. *Front Immunol.* 2014;5:614.
5. Mantovani A, Sozzani S, Locati M, Allavena P, Sica A. Macrophage polarization: Tumor-associated macrophages as a paradigm for polarized M2 mononuclear phagocytes. *Trends Immunol.* 2002;23(11):549–55.
6. Luo M, Zhao F, Cheng H, Su M, Wang Y. Macrophage polarization: An important role in inflammatory diseases. *Front Immunol.* 2024;15:1352946.
7. Strizova Z, Benesova I, Bartolini R, Novysedlak R, Cecdlova E, Foley LK, et al. M1/M2 macrophages and their overlaps—myth or reality? *Clin Sci.* 2023;137(16):1067–93.
8. Li S, Huo C, Liu A, Zhu Y. Mitochondria: A breakthrough in combating rheumatoid arthritis. *Front Med.* 2024;11:1439182.

9. De Benedittis G, Latini A, Morgante C, Perricone C, Ceccarelli F, Novelli G, et al. The dysregulation of mitochondrial homeostasis-related genes could be involved in the decrease of mtDNA copy number in systemic lupus erythematosus patients. *Immunol Res.* 2024;72(5):1384–92.
10. Barrera MJ, Aguilera S, Castro I, Carvajal P, Jara D, Molina C, et al. Dysfunctional mitochondria as critical players in the inflammation of autoimmune diseases: Potential role in Sjögren's syndrome. *Autoimmun Rev.* 2021;20(9):102867.
11. Kowalczyk P, Sulejczak D, Kleczkowska P, Bukowska-Osko I, Kucia M, Popiel M, et al. Mitochondrial oxidative stress—a causative factor and therapeutic target in many diseases. *Int J Mol Sci.* 2021;22:13384.
12. Hu MM, Shu HB. Mitochondrial DNA-triggered innate immune response: Mechanisms and diseases. *Cell Mol Immunol.* 2023;20(12):1403–12.
13. Jiao Y, Yan Z, Yang A. Mitochondria in innate immunity signaling and its therapeutic implications in autoimmune diseases. *Front Immunol.* 2023;14:1160035.
14. Jiang J, Zhao M, Chang C, Wu H, Lu Q. Type I interferons in the pathogenesis and treatment of autoimmune diseases. *Clin Rev Allergy Immunol.* 2020;59(2):248–72.
15. Drougkas K, Skarlis C, Mavragani C. Type I interferons in systemic autoimmune rheumatic diseases: Pathogenesis, clinical features and treatment options. *Mediterr J Rheumatol.* 2024;35(4):365–80.
16. Funes SC, Rios M, Escobar-Vera J, Kalergis AM. Implications of macrophage polarization in autoimmunity. *Immunology.* 2018;154(2):186–95.
17. Signes A, Fernandez-Vizarra E. Assembly of mammalian oxidative phosphorylation complexes I–V and supercomplexes. *Essays Biochem.* 2018;62(3):255–70.
18. Prasun P. Mitochondrial dysfunction in metabolic syndrome. *Biochim Biophys Acta Mol Basis Dis.* 2020;1866(10):165838.
19. Bae HR, Shin SK, Han Y, Yoo JH, Kim S, Young HA, et al. D-Allulose ameliorates dysregulated macrophage function and mitochondrial NADH homeostasis, mitigating obesity-induced insulin resistance. *Nutrients.* 2023;15(19):4218.
20. Bae HR, Shin SK, Yoo JH, Kim S, Young HA, Kwon EY. Chronic inflammation in high-fat diet-fed mice: Unveiling the early pathogenic connection between liver and adipose tissue. *J Autoimmun.* 2023;139:103091.
21. Faas MM, De Vos P. Mitochondrial function in immune cells in health and disease. *Biochim Biophys Acta Mol Basis Dis.* 2020;1866(10):165845.
22. De Barcelos IP, Troxell RM, Graves JS. Mitochondrial dysfunction and multiple sclerosis. *Biology.* 2019;8(2):37.
23. Martinez FO, Gordon S. The M1 and M2 paradigm of macrophage activation: Time for reassessment. *F1000Prime Rep.* 2014;6:13.
24. Green DS, Young HA, Valencia JC. Current prospects of type II interferon  $\gamma$  signaling and autoimmunity. *J Biol Chem.* 2017;292:13925–33.
25. De George DJ, Ge T, Krishnamurthy B, Kay TWH, Thomas HE. Inflammation versus regulation: How interferon-gamma contributes to type 1 diabetes pathogenesis. *Front Cell Dev Biol.* 2023;11:1205590.
26. Kiritsy MC, McCann K, Mott D, Holland SM, Behar SM, Sasseti CM, et al. Mitochondrial respiration contributes to the interferon gamma response in antigen-presenting cells. *eLife.* 2021;10:e65109.
27. Wang F, Zhang S, Jeon R, Vuckovic I, Jiang X, Lerman A, et al. Interferon gamma induces reversible metabolic reprogramming of M1 macrophages to sustain cell viability and pro-inflammatory activity. *EBioMedicine.* 2018;30:303–16.
28. Kelly B, O'Neill LA. Metabolic reprogramming in macrophages and dendritic cells in innate immunity. *Cell Res.* 2015;25(7):771–84.
29. Bae HR, Leung PS, Tsuneyama K, Valencia JC, Hodge DL, Kim S, et al. Chronic expression of interferon-gamma leads to murine autoimmune cholangitis with a female predominance. *Hepatology.* 2016;64(4):1189–201.
30. Hodge DL, Berthet C, Coppola V, Kastenmüller W, Buschman MD, Schaughency PM, et al. IFN-gamma AU-rich element removal promotes chronic IFN-gamma expression and autoimmunity in mice. *J Autoimmun.* 2014;53:33–45.
31. Bae HR, Hodge DL, Yang G, Leung PS, Chodisetti SB, Valencia JC, et al. The interplay of type I and type II interferons in murine autoimmune cholangitis as a basis for sex-biased autoimmunity. *Hepatology.* 2017;67(4):1408–19.
32. Bae HR, Leung PS, Hodge DL, Fenimore JM, Jeon SM, Thovarai V, et al. Differential expression of IFN- $\gamma$  results in distinctive mechanistic features linking chronic inflammation, gut dysbiosis, and autoimmune diseases. *J Autoimmun.* 2020;111:102436.
33. Fenimore JM, Springer DA, Romero ME, Edmondson EF, McVicar DW, Yanpallewar S, et al. IFN- $\gamma$  and androgens disrupt mitochondrial function in murine myocytes. *J Pathol.* 2023;260(4):276–88.
34. Bethunaickan R, Berthier CC, Ramanujam M, Sahu R, Zhang W, Sun Y, et al. A unique hybrid renal mononuclear phagocyte activation phenotype in murine systemic lupus erythematosus nephritis. *J Immunol.* 2011;186(8):4994–5003.

35. Arazi A, Rao DA, Berthier CC, Davidson A, Liu Y, Hoover PJ, et al. The immune cell landscape in kidneys of patients with lupus nephritis. *Nat Immunol.* 2019;20(7):902–14.
36. Wu D, Sanin DE, Everts B, Chen Q, Qiu J, Buck MD, et al. Type 1 interferons induce changes in core metabolism that are critical for immune function. *Immunity.* 2016;44:1325–36.
37. Viola A, Munari F, Sánchez-Rodríguez R, Scolaro T, Castegna A. The metabolic signature of macrophage responses. *Front Immunol.* 2019;10:1462.
38. Rabanal-Ruiz Y, Otten EG, Korolchuk VI. mTORC1 as the main gateway to autophagy. *Essays Biochem.* 2017;61(6):565–84.
39. Su X, Yu Y, Zhong Y, Giannopoulou EG, Hu X, Liu H, et al. Interferon- $\gamma$  regulates cellular metabolism and mRNA translation to potentiate macrophage activation. *Nat Immunol.* 2015;16(8):838–49.
40. Bae H, Guan JL. Suppression of autophagy by FIP200 deletion impairs DNA damage repair and increases cell death upon treatments with anticancer agents. *Mol Cancer Res.* 2011;9(10):1232–41.
41. Hewitt G, Korolchuk VI. Repair, reuse, recycle: The expanding role of autophagy in genome maintenance. *Trends Cell Biol.* 2017;27(5):340–51.
42. Raj S, Chandel V, Kumar A, Kesari KK, Asthana S, Ruokolainen J, et al. Molecular mechanisms of interplay between autophagy and metabolism in cancer. *Life Sci.* 2020;259:118184.
43. Yang Y, Klionsky DJ. Autophagy and disease: Unanswered questions. *Cell Death Differ.* 2020;27(3):858–71.
44. Chu Y, Chang Y, Lu W, Sheng X, Wang S, Xu H, et al. Regulation of autophagy by glycolysis in cancer. *Cancer Manag Res.* 2020;12:13259–71.
45. Yin H, Wu H, Chen Y, Zhang J, Zheng M, Chen G, et al. The therapeutic and pathogenic role of autophagy in autoimmune diseases. *Front Immunol.* 2018;9:1512.
46. Sharma LK, Lu J, Bai Y. Mitochondrial respiratory complex I: Structure, function and implication in human diseases. *Curr Med Chem.* 2009;16(10):1266–77.
47. Mishra SR, Mahapatra KK, Behera BP, Patra S, Bhol CS, Panigrahi DP, et al. Mitochondrial dysfunction as a driver of NLRP3 inflammasome activation and its modulation through mitophagy for potential therapeutics. *Int J Biochem Cell Biol.* 2021;136:106013.
48. Chen Y, Ye X, Escames G, Lei W, Zhang X, Li M, et al. The NLRP3 inflammasome: Contributions to inflammation-related diseases. *Cell Mol Biol Lett.* 2023;28(1):1–27.
49. Kim J, Kim HS, Chung JH. Molecular mechanisms of mitochondrial DNA release and activation of the cGAS-STING pathway. *Exp Mol Med.* 2023;55(4):510–9.
50. Carroll D, Turner JR, Hellowell JC. Heart rate and oxygen consumption during active psychological challenge: The effects of level of difficulty. *Psychophysiology.* 1986;23(2):174–81.
51. Kremer LS, Rehling P. Coordinating mitochondrial translation with assembly of the OXPHOS complexes. *Hum Mol Genet.* 2024;33:R47–R52.
52. Pawar K, Kawamura T, Kirino Y. The tRNA(Val) half: A strong endogenous Toll-like receptor 7 ligand with a 5'-terminal universal sequence signature. *Proc Natl Acad Sci USA.* 2024;121:e2319569121.